SOFT MATERIALS AND BIOMATERIALS UNDER PRESSURE

Putting the Squeeze on Biology

S.M. GRUNER
Physics Department &
Cornell High Energy Synchrotron Source (CHESS)
Cornell University
Ithaca, NY 14853-2501, USA

1. Introduction

Soft-matter macromolecular assemblies include proteins; biomembranes; surfactant, lipid, and block-copolymer mesophases; cellular cytoskeletal networks; and other large-molecule assemblies found in living systems. These systems generally differ from small-molecule systems in that the molecules have many "parts", each of which may have a huge number of conformational substates. The free energies of different substates often differ only slightly, even though the 3-dimensional molecular structures may differ greatly. A dramatic example is the two substate ensembles represented by a protein in its native and unfolded states. Unfolding may occur with only modest changes in environmental conditions (e.g., temperature, solvent conditions) and with extremely small transition enthalpies. Despite the small energy change, the structures, and, more importantly, functionality of the folded and unfolded protein could hardly be more different.

Pressure is one of the fundamental environmental variables that affect conformational substates. In fact Percy Bridgman, considered to be the father of modern high-pressure science, observed in 1914 that 5000 atmospheres (1atmosphere ≈ 1 bar ≈ 10^5 Pa) of pressure would coagulate (i.e., unfold) egg white [1]. Pressure-induced protein unfolding is now recognized to be a general phenomenon [2]. The free energies of folded and unfolded proteins differ only slightly, which accounts for why work of pressurization -- the pressure-volume change product $\Delta(PV)$ -- required to accomplish this phase transformation is very small. Even smaller free energy changes are usually associated with the conformational substate alterations of a folded protein as it undergoes functional activity. This naturally brings up questions:

1. Does pressure in the range of up to several kbar (which we call *medium pressure*) alter the ensemble of conformational substates in a macromolecular soft-matter assembly?

2. Since the ensemble of conformational substates under a given set of environmental conditions greatly determines functional activity for many

A. Katrusiak and P. McMillan (eds.), High-Pressure Crystallography, 543–556.

such systems (e.g., proteins, biomembranes), does it follow that medium pressure affects soft-matter function?

The literature is replete with observations that medium pressure has extraordinary effects on soft-matter macromolecular systems [3-8]. Pressure is known to change protein chemical kinetic and equilibrium constants of multimeric associations, folding profiles and ligand binding. It greatly alters biomembrane permeability. Cellular metabolism, cellular morphology, and viral infectivity can be greatly affected. Further, these effects are often observed in the medium pressure regimes encountered in the biosphere, i.e., about a kbar in the deepest ocean trenches and up to several kbar, if one accepts ideas about living bacterial organisms in ground waters in the top several km of the earth's crust.

Although the catalog of observed medium pressure effects is long, a survey of the literature reveals only a rudimentary understanding of the fundamental mechanisms responsible for the effects. Why is this so? If conformational changes are involved, then an understanding must begin with observation of the ways in which pressure affects macromolecular structure. The simple fact of the matter is that most high-pressure studies to date do not determine macromolecular structure. Typically, chemical or spectroscopic techniques are used to infer the effects of pressure. Conformational substate changes can be either *local* (e.g., rotation of a single amino acid side-group) or *global* (e.g., allosteric response of a protein to the binding of multiple ligands – hemoglobin is a classic example [9]). While chemical and spectroscopic methods can sometimes be used to infer local conformations, they do not directly yield structure.

The ideal tool for determination of global changes in structure is, of course, x-ray diffraction. Having already noted that there are a huge number of medium pressure effects on myriad protein systems at biologically relevant pressures, the reader may be surprised to find that only a few medium pressure protein crystallographic studies have been performed (see [10-16] and references therein). The structures of only two proteins, lysozyme [11, 12, 14] and myoglobin [16], have been solved at medium pressure. The paucity of structural studies is a consequence of the difficulties, until very recently, in performing protein crystallography at medium pressures (discussed below). Thus, medium pressure macromolecular crystallography is topical and ripe for exploration.

2. Molecular Assemblies with Parts

A distinguishing feature of soft-matter macromolecular assemblies is that they have distinct "parts". In a protein, these might be the various secondary structural elements (alpha helices and the like) that lead to tertiary structure, which, in turn, lead to domains in quaternary structure. In a lipid-water lyotrope, the parts include the hydrocarbon chain region, the hydrophilic headgroup sheet and the water that makes up the mesophase. These parts may each have different compressibilities, in which case pressure will lead to movements of the parts relative to one another and

changes in the overall structure and shape of the assembly. In many cases, the overall structure of the assembly results from the way in which the parts are held together by a carefully balanced set of interactions (salt bridges, hydrogen bonding, van der Waals interactions, etc.). Many of these interactions are also pressure sensitive, which may lead to a shift of the balance and a change in structure.

The relevant feature is not the *absolute* magnitude of the compressibility or change in an interaction, but the *relative* change leading to significant structural change. A good analogy is the bimetallic strip in a thermal sensor. The strip can execute a large bending movement with temperature, even though the absolute changes in linear expansion of the two metals might be small, because of the relative change in thermal expansion is amplified by the way the two metal strips are bonded together.

An explanation of the effects of medium pressure on many biological systems will require understanding pressure-induced structural alteration in proteins. The way that the parts of a protein functionally interact is often difficult to understand from the static high-resolution structure. For this reason, I'll illustrate pressure-induced structural changes with examples of structurally simpler lipid systems in which the pressure effects can be more readily understood in terms of the effects on the parts of the lipid assembly.

3. Thermally-Induced Lipid Mesomorphism

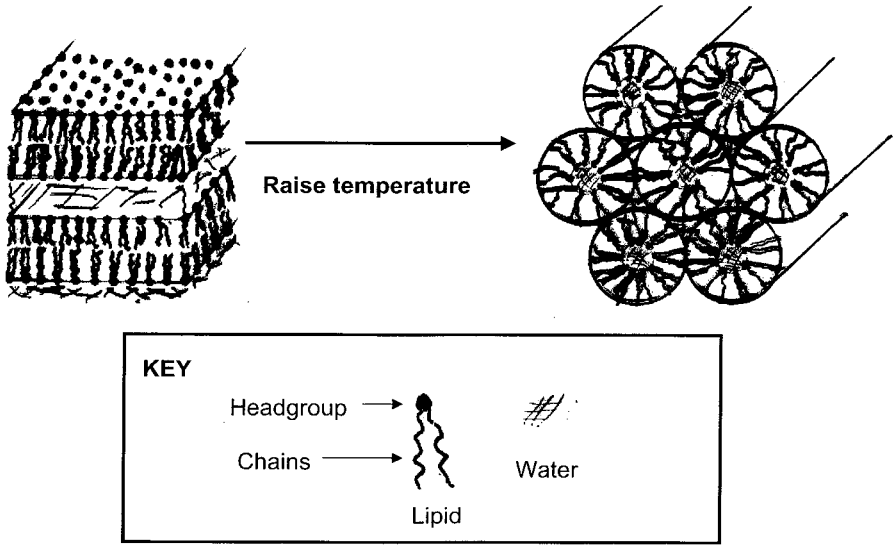

Figure 1.The L_α and H_{II} phases are commonly seen when diacyl phospholipids are dispersed in excess water. In the L_α phase (left) the lipids form bilayer sheets that stack with intervening water layers. In the H_{II} phase (right) the lipids form into water-cored tubes packed on a 2-dimensional hexagonal lattice. The circles are drawn to guide the eye. Phase transitions between the phases are driven by temperature. Both phases can coexist with an excess, bulk water phase.

It is instructive to first understand the temperature-induced behavior of our lipid system before considering the pressure-induced behavior. Lipid-water dispersions have extraordinarily rich liquid crystalline phase behavior [17, 18]. The L_α - H_{II} phase transition (Figure 1) is of particular interest since it has been the foundation for studies on the spontaneous curvature of the monolayers that make up the bilayers in biomembranes [19-24]. In brief, a typical biomembrane is about half (by weight) polar lipid and half protein and associated carbohydrates. In eukaryotic cells, the polar lipids are most commonly phospholipids with two hydrocarbon tails. Although there may be hundreds of chemically distinct lipids in any given membrane, the lipids divide into two classes, depending on the equilibrium phases that occur when a given, chemically pure membrane lipid is dispersed in water under physiological conditions. Very roughly, half of the lipids form L_α phases and half form H_{II} phases. Further, the lipids that form H_{II} phases tend to revert to L_α phases upon cooling; similarly, L_α phases tend to form H_{II} phases upon heating.

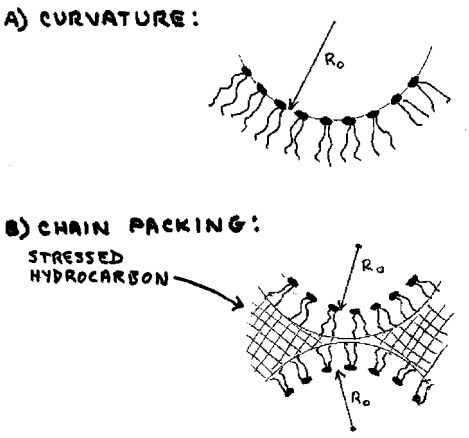

Figure 2. The frustrated competition between monolayer spontaneous curvature and hydrocarbon packing dominates the lipid mesophase behavior.

The physics underlying the L_α - H_{II} phase transition has been intensively investigated and is now reasonably well understood [19-24]. It is the consequence of the geometrically frustrated competition between the spontaneous curvature of the lipid monolayers that make up the phases and the entropically-driven propensity for the hydrocarbon chains to exist in a translationally invariant environment, subject to the constraints of shielding the hydrocarbon chains from exposure to water and the polar lipid headgroups in contact with water. To visualize the frustration, assume the lipid monolayer free-energy with respect to bend is minimized when it is rolled into a cylinder of radius $R = R_0$ (Figure 2a), that is to say R_0 is the value of R that self-consistently minimized the elastic bending energy. Liquid crystal elastic theory shows that, to lowest nontrivial order, the energy per unit area to bend the layer goes as $(1/R - 1/R_0)^2$, that is to say it costs free energy to bend the layer away from R_0. However, the hydrocarbon also has to be shielded from exposure to water, so adjacent monolayers are opposed to one another to form bilayers. If the monolayers are locally flat (as in the L_α phase) the hydrocarbon chain bilayer is of uniform thickness throughout. However, if the opposed monolayers are highly curved, the hydrocarbon layers curl away from one another, as shown by the cross-hatched area in Figure 2b, forcing the hydrocarbon chains to stretch to fill the gap.

This is more readily seen in Figure 3b, where the lipid monolayers are seen to have rolled into cylinders of uniform curvature, which then pack into a 2-dimensional, hexagonal lattice. If the cylinders have radius R_0, then they are elastically relaxed and, by definition, the free energy with respect to bend is minimized. However, the hydrocarbon chains have to stretch to reach into the triangular area between the three cylinders. This stretching reduces the number of configurations available to the hydrocarbon chains and raises their free energy – this is called the hydrocarbon packing energy. This leads to the unavoidable frustration: relaxing the bending energy by curling opposed monolayers raises the free energy of the hydrocarbon volume. An alternative is for the monolayers to flatten out into a L_α phase, thereby raising the bending energy, but lowering the hydrocarbon packing free energy. Which of these two frustrated geometries is chosen depends on which results in overall lower composite free energy. In other words, the phase that is observed is the answer to the question of does it cost more energetically to bend or to uniformly fill the hydrocarbon volume?

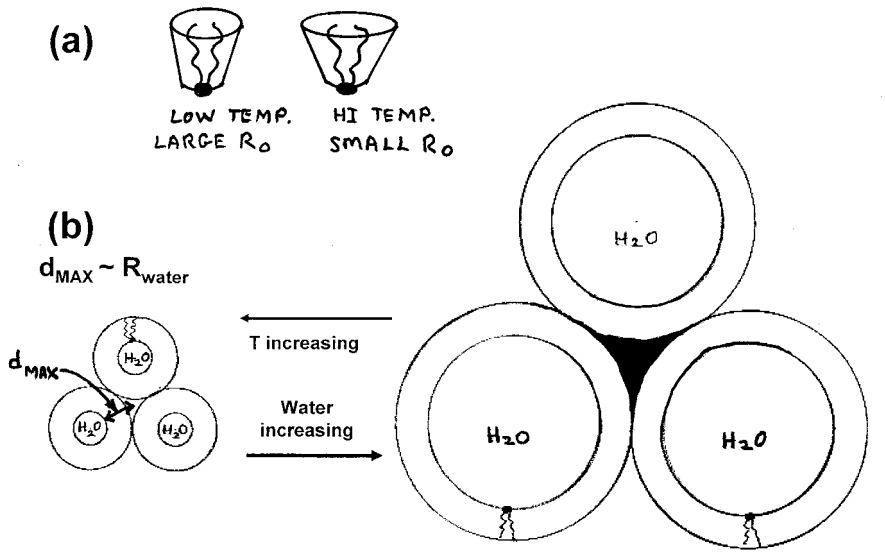

Figure 3.The L_α and H_{II} phases are commonly seen when diacyl phospholipids are dispersed in excess water. In the L_α phase (left) the lipids form bilayer sheets that stack with intervening water layers. In the H_{II} phase (right) the lipids form into water-cored tubes packed on a 2-dimensional hexagonal lattice. The circles are drawn to guide the eye. Phase transitions between the phases are driven by temperature. Both phases can coexist with an excess, bulk water phase.

The spontaneous curvature is temperature dependent. As illustrated in Figure 3a, increasing temperature increases the number of *gauche* rotamers excited in the hydrocarbon chains and causes the ends of the chains to splay more widely. These are liquid crystalline structures, so the molecules are constantly fluctuating and rotating around their long axis. If we represent the time-averaged volume swept out

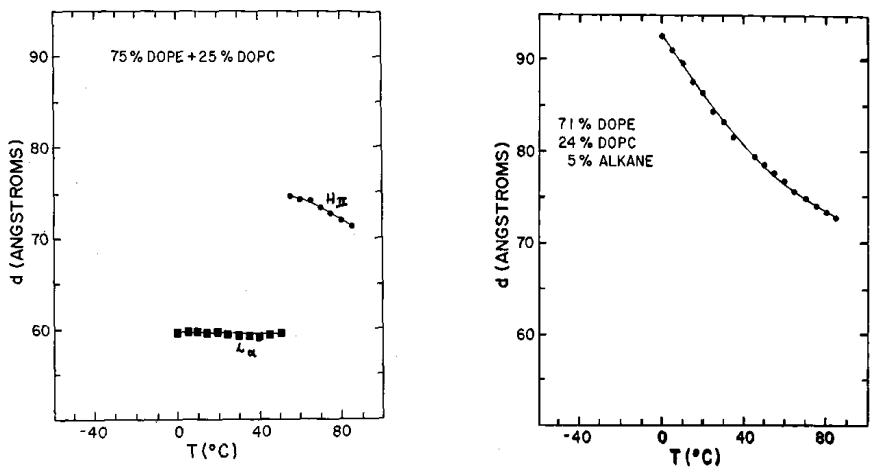

Figure 4. (a) A mixture of 3:1 of the lipids DOPE and DOPC forms L_α phases (squares) from 0°C up to about 55°C, above which the H_{II} phase (circles) is observed. The graphs show the unit cell dimensions, i.e., the bilayer repeat distance in the L_α phase and the cylinder center-to-center distance in the H_{II} phase. Data below 0°C is influenced by freezing water and is not shown. The addition of a few weight percent of a light alkane relieves the hydrocarbon packing stress (b) and allows the spontaneous curvature to be expressed as an H_{II} phase over the entire region.

by the molecule, it looks like a truncated cone. Higher temperatures result in more disordered chain ends, which correspond to cones with a wider base. When packed side-by-side, these tile a smaller radius cylinder than the narrower-based cones corresponding to lower temperatures. The equilibrium cylinder radius tiled with such cones *is* the spontaneous radius of curvature. So *higher* temperatures correspond to *smaller* spontaneous radii of curvature.

What is actually observed, as measured by x-ray diffraction, is that the H_{II} phase cylinders shrink as the temperature rises, i.e., the mesophase goes from the right to the left sides of Figure 3a. It should be mentioned that this is true only when the mesophase is in equilibrium with excess bulk water, i.e., fully hydrated. In this case, the water volume in the cylinder cores is not a constraint. When the cylinders grow, they simply pull in more water from the coexisting bulk; when they shrink, they reject water into that bulk. The cross-sectional area per cylinder is also not a constraint, since a liquid crystalline monolayer is really a 2-dimensional fluid. Thus, as the cylinders shrink in radius, they are free to elongate to preserve the cross-sectional lipid molecular area.

A final consideration is that it can be shown that the free energy cost of filling the triangular area between the cylinders grows with increasing cylinder radius. Thus the hydrocarbon packing energy per lipid increases in going from the left to the right of Figure 3b.

We are now prepared to understand the behavior of a fully hydrated L_α - H_{II} phase transition. Figure 4a shows the unit cell dimensions and the phases observed in a dispersion of a mixture of two lipids, called DOPE and DOPC [35]. The L_α phase is observed up to about 55˚C, above which the lipid dispersion transforms to H_{II} phase. The largest H_{II} phase unit cell occurs at the L_α - H_{II} phase transition temperature. As the temperature increases, the H_{II} unit cell, i.e., the lipid tube radii, shrink. This is simply a manifestation of the thermally-driven decrease in the lipid monolayer radius of spontaneous curvature discussed above. The way to think about this is to imagine starting in the H_{II} phase, where the overall free energy is dominated by minimizing the energy of bending the lipid monolayers, and then lowering the temperature slowly from say, 80˚C. As the temperature falls, the lipid tube spontaneous radius of curvature rises, so the tubes grow, as manifest by a progressive increase in the H_{II} phase unit cell size. But recall that the energetic cost of the hydrocarbon packing energy, i.e., filling the triangle of Figure 3b, rises with increasing cylinder radius. Thus, decreasing the temperature leads to progressively larger and larger frustrated free energy associated with packing the hydrocarbon chains. At about 55˚C, the overall free energy is minimized by packing lipids in a different geometry, such as the L_α phase, in which the curvature energy is frustrated but the hydrocarbon chains are relaxed.

This scenario of what drives the phase transition is further supported by a simple experimental trick: If a few weight per cent of a hydrophobic oil, such as decane, is added, it partitions into the hydrocarbon zone and relieves the packing stress by preferentially partitioning in the triangular region between the cylinders of Figure 3b. This has been directly verified by neutron diffraction studies with deuterated decane [25]. The effect is to remove the frustration of hydrocarbon packing in the H_{II} phase, with the result that the L_α - H_{II} phase transition now disappears (Figure 4b). Rather, the H_{II} phase cylinder simply continue to grow as the temperature drops.

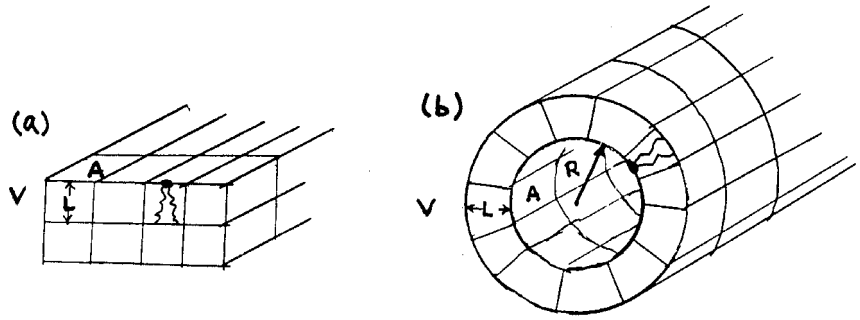

Figure 5. In the L_α phase (a), the time-averaged lipid volume, *V*, is simply the monolayer thickness, *L*, times the molecular headgroup area, *A*. For a given value of *V*, variation in *L* is matched by an inverse variation in A. By contrast, in the H_{II} phase (b), for a given *V*, *A* and *L* can change independently by changing the radius of the annular shell tiled by the lipid molecules.

The change in spontaneous radius of curvature is a simple manifestation of thermally-induced disorder in the hydrocarbon monolayer. It had been known for many years that the lipid monolayer thickness shrinks at a rate of about 0.01 Å/°C with increasing temperature due to increasing disorder in the hydrocarbon chains. In the L_α phase, simply due to the geometry of the phase (Figure 5a), the average lipid molecular volume, V, is the product of the lipid headgroup molecular cross-sectional area, A, times the monolayer thickness, L: $V = AL$. In other words, in so far as the molecular volume is nearly constant, changes in A and L vary inversely to one another. However, the tubular geometry of the H_{II} phase (Figure 5b) has an additional degree of freedom so it is possible to change the thickness of the monolayer and the headgroup area independently at nearly constant molecular volume by changing the radius of the cylinder. For the sake of illustration, assume typical lipid values of $V = 1250$ Å^3, and L changing from 20.2 Å to 20.0 Å over a 20°C temperature rise. In the L_α phase, this results in thinning of the bilayer by 0.4 Å. However, in the H_{II} phase, with $V = 1250$ Å^3 and a typical headgroup area of 50 Å^2, a decrease in lipid monolayer thickness from 20.2 Å to 20.0 Å results in a change of cylinder diameter of 5.4 Å. The cylindrical geometry amplifies the small change in monolayer thickness into an almost factor of ten larger change in cylinder radius! This explains why the unit cell of the L_α phase changes so little in temperature relative to the H_{II} phase (Figure 4a).

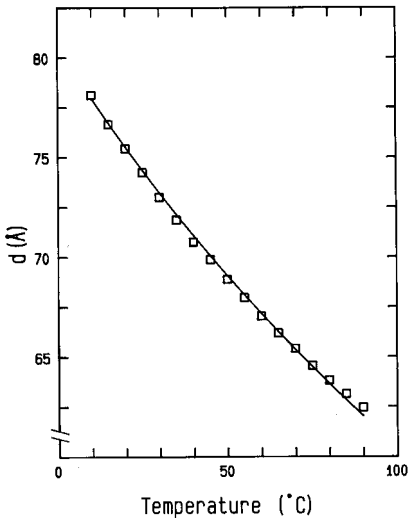

Figure 6. The measured unit cell repeat spacing (squares) of a DOPE-excess water phase versus temperature is well-modeled by the calculated values (smooth line). From reference [26].

A more precise calculation, taking into account the *measured* thermal dependence of V, A and L and the hexagonal Wigner-Seitz cell of the H_{II} phase is shown in Figure 6. The data (squares) are well modeled by the calculated unit cell size (smooth line) with *zero* free parameters [26].

4. Pressure-Induced Lipid Mesomorphism

We are now prepared to examine the pressure effects on these same lipid-water dispersions. First, let's *predict* what we expect to see, based upon what we've learned from the thermal behavior. Pressure acts to squeeze out free molecular volume. In the lipid system, the most compressible part is the hydrocarbon layer. This isn't too surprising, since the compressibility of water is about 50 ppm/bar, whereas the compressibility of *n*-octane is about 130 ppm/bar. The many *cis*

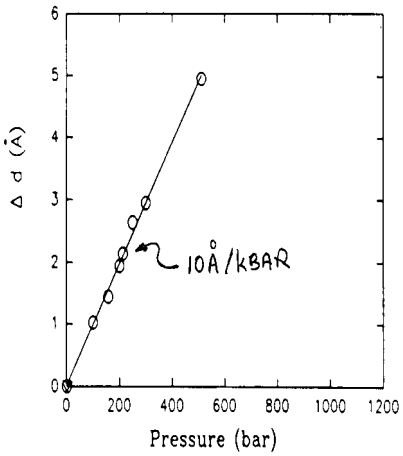

Figure 7. The unit cell spacing of an excess-water H_{II} phase increases dramatically with pressure.

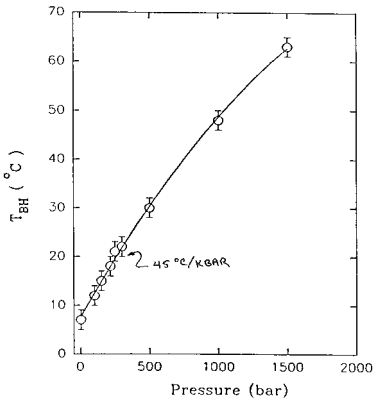

Figure 8. The excess-water DOPE L_α-H_{II} phase transition temperature, T_{BH}, varies dramatically with pressure.

rotamers in a melted hydrocarbon chain cause the chains to pack poorly and lead to molecular voids that are readily squeezed out by pressure. Translated to a lipid monolayer, this suggests, unsurprisingly, that the system reacts to increasing pressure much as it would to falling temperature, i.e., the lipid monolayer thickness increases with increasing pressure as *cis* rotamers are squeezed out and the chains become more fully *trans*. Thus, our first prediction is that the unit cell of the H_{II} phase in excess water will *increase* with increasing pressure. This is shown in Figure 7 [27]. This seemingly counter-intuitive result is readily understood by the realization that the increase in unit cell size is really a decrease in overall system volume, once the molecular volumes of both lipid and water are taken into account [28]. Further, the coefficient of unit cell increase is predictably large, 10 Å/kbar, for exactly the same reason that the H_{II} phase unit cell thermal coefficient is large – it actually corresponds to a factor of ten smaller change in the thickness of the monolayer wall of the lipid tube.

We also have learned that the L_α - H_{II} phase transition is dominated by the frustration between expression of the monolayer spontaneous curvature and hydrocarbon packing, and that this frustration is linked to the H_{II} phase tube diameter. Since increasing pressure leads to increasing tube diameter, we would predict that the L_α - H_{II} phase transition temperature would increase with pressure. This is shown in Figure 8. In fact, this first order phase transition has one of the largest coefficients of pressure sensitivity found in any non-gaseous condensed matter system.

Detailed studies of the pressure dependence of the L_α - H_{II} phase system may be found in the literature [27, 29-31].

In summary, we have analyzed the structure of this complex macromolecular assembly and the way in which its parts interact to produce the system behavior.

Once this is done, then an understanding of the relative anisotropic compressibilities of the parts lets us understand the pressure-induced behavior of the system. The specific details peculiar to lipid-water dispersions will be quite different than the details in other macromolecular assemblies, such as proteins. But the overall strategy and approach should be quite similar.

5. High Pressure X-ray Cells

Not surprisingly, the greatest impediment to doing x-ray experiments at medium pressure is the difficulty of working with x-ray transparent pressure cells. The lipid studies described above involve small angle x-ray scattering (SAXS) from powder pattern dispersions. This is a relatively forgiving experimental geometry readily satisfied by simple beryllium window cells [27, 30]. Medium pressure high-resolution protein crystallography is much more challenging for several reasons: Protein crystals are small, in normal oscillation x-ray diffraction the crystals must be precisely rotated in the x-ray beam, and relatively weak Bragg reflections must be quantitatively recorded out to wide angles. The difficulty of performing medium pressure x-ray crystallography has certainly been the single most important reason for the paucity of studies.

The first high resolution protein structure to be solved at 1 kbar was that of hen egg white lysozyme by Kundrot and Richards [11, 12] in 1986-1987. They employed a beryllium rod, about 2.5 centimeters long and about half a centimeter in diameter, with a dead-ended hole. The crystal was inserted into the hole and the rod was then screwed into a high-pressure o-ring seal fixture that mounted directly on a standard crystallography goniometer. Stainless steel syringe tubing was used to convey high pressure fluid to the crystal.

Major difficulties with this type of pressure chamber include limited pressure (although the seal arrangement has been modified to reach 2 kbar [32]), the difficulty of aligning the crystal as it is not visible when in the cell, a high background and absorption due to the beryllium, and the need to work with beryllium, which is quite toxic. The most troublesome aspect, however, is that the presence of beryllium powder pattern rings makes it very difficult to acquire data to better than about 2 Å resolution.

An alternative method follows from work by Thomanek et al. [10] who froze myoglobin crystals to liquid nitrogen temperature under high pressure. They showed that a substate is frozen in place and remains even after if the pressure is removed. The substate relaxed when the crystals were warmed well above 100K. This suggested that pressure-induce structural alterations are preserved at low temperatures, even if the pressure is removed.

Urayama et al. [16] compared myoglobin structural data acquired using a modified Kundrot-Richards cell and crystals that were deep-frozen while under pressure. To do the latter, the crystals were pressurized in isopentane in a high-pressure fixture,

which was then immersed in liquid nitrogen. The pressure was then removed and the fixture disassembled under liquid nitrogen. Isopentane at liquid nitrogen temperatures is sufficiently soft that the protein crystals could be extracted with microforceps. After extraction, crystallography was performed using standard cryostream apparatus. In order to observe collective structural alterations, it was first necessary to devise a simple numerical procedure to remove the isotropic elastic expansion that occurred in the frozen crystals when pressure was released. The resulting structures were compared to those acquired under (a) room temperature and room pressure, (b) room temperature and high pressure, and (c) low temperature and high pressure. The results showed that structural alterations that were frozen in at high pressure were largely preserved even if the pressure was removed.

The experimental significance of this work is that it demonstrated that pressure-induced structural changes in myoglobin can be determined without having to perform the crystallography at high pressure. This vastly simplifies the pressure experiment. If this turns out to be a generally true for proteins, then study of the effects of pressure on proteins can be routinely performed.

A third method to perform the crystallographic experiment is to use a diamond anvil cell (DAC). Because the DAC exit angle is limited and because the diamonds absorb x-rays, the experiments typically utilize higher energy x-rays. Katrusiak and Dauter performed some of the first DAC protein studies [13]. More recently, Fourme and colleagues have used a DAC to collect crystallographic data on lysozyme and on a virus crystal [14, 15] at pressures exceeding 2 kbar. Radiation damage will become an issue unless the DAC is cooled to liquid nitrogen temperatures.

6. Medium Pressure Effects on Protein Structure

The field of protein structure under pressure is in its infancy. To date, only two proteins, lysozyme and myoglobin, have had medium pressure, high resolution structural determinations. Given the huge diversity in protein structural motifs and mechanisms of operation, it would be dangerous to draw general conclusions from only two proteins.

Both lysozyme and myoglobin are robust, compact proteins for which pressure induced alterations would be expected to be small. Even so, collective displacements of protein parts were observed in both cases.

In the case of lysozyme [11, 12], the intrinsic compressibility was 4.7×10^{-3}/kbar (see also [13, 14]). Protein domain 1 (residues 1-39, 89-129) had a compressibility of 5.7×10^{-3}/kbar, while domain 2 (residues 40-88) was almost incompressible. Note that domain 1 is mostly α helical while domain 2 is mostly composed of β sheets. Shifts in atomic positions were generally less than 1 Å, and most backbone atoms shifted by an RMS value of about 0.12 Å. Though small, this collective shift was

well above the estimated detectable limit of 0.06 Å. The unit cell *a* axis decreased and the *c* axis increased slightly upon pressurization. This anisotropy already suggests interesting structural changes.

In the case of myoglobin, the detectable limit for shifts was shown to conservatively be about 0.1 Å. Myoglobin consists of eight α-helical segments, labeled A through H, connected by loops. The largest collective effects were a sliding of the F helix, an opening of the loop connecting the C & D helices, and an overall contraction of the primary protein matrix. Urayama [32] discussed these changes in terms of the known spectroscopy of O_2 and CO ligand binding in myoglobin, as determined from high pressure spectroscopy.

The observed collective pressure-induced structural shifts in both lysozyme and myoglobin are small. It would be a mistake to assume that the shifts are not significant. Myoglobin, especially, illustrates the fallacy of assuming that small-level shifts on the order of a few tenths of an Angstrom are insignificant: Very small shifts of specific groups near the ligand binding site are known to occur upon binding and to have large effects on the ligand binding behavior. Small displacements may have large consequences. I suspect that other proteins, when examined, will display a range of structural shifts, ranging from relatively slight to large.

Lysozyme and myoglobin are both monomeric aqueous proteins. Other assemblies of interest include multimeric and fibrous proteins and membrane proteins. Membrane proteins, in particular, have additional mechanisms for pressure-induced effects because their structure is intimately coupled to imbedding lipid bilayers. Perhaps it won't surprise the reader that certain membrane proteins are thought to be responsive to the lipid monolayer spontaneous curvature [33]. But, as noted earlier, the spontaneous curvature is a sensitive function of pressure. Therefore, it may well be that pressure effects on membrane proteins are additionally mediated by changes in the lipid bilayer environment [34].

7. Perspective

The world is full of important soft-matter known to be responsive to medium pressure. Yet there are relatively few structural studies on the effects of medium pressure on soft matter. Why is this so? Scientists are inherently very conservative and tend to stick to their own specific scientific communities. Relatively few scientists familiar with high pressure and x-ray techniques also work with soft matter. Another factor may be the bias that structural effects should be small in the medium pressure range because soft matter is typically highly incompressible and, therefore, the change in molecular volume must be very small. As I have illustrated, above, the large number of substates in soft matter allows large (or in some case small but highly consequential) changes in structure to occur with small changes in molecular volume. A final reason for the paucity of studies is that relatively easy experimental methods for structural determinations of soft matter under medium

pressure are just now emerging – an example is the observation that pressure-induced changes in protein crystals may be frozen in place.

All these reasons simply argue the obvious: Most of the natural world remains to be explored. The future will be very interesting.

8. Acknowledgements

I am grateful to many colleagues with whom I have worked over the years to investigate the effects of pressure on soft-matter. I wish to especially acknowledge Peter So, Shyamsunder Erramilli, Manfred Kriechbaum, Onuttom Narayan, Fred Osterberg, George Phillips Jr., Mark Tate, Richard Templer, David Turner and Paul Urayama. I am thankful to the U.S. Department of Energy, the National Institutes of Health and the Office of Naval Research for support.

9. References

1. Bridgman, P.W. (1914) The coagulation of albumen by pressure, *J. Biol. Chem*., **19**, 511-512.
2. Royer, C.A. (2002) Revisiting volume changes in pressure-induced protein unfolding, *Biochimica et Biophysica Acta* **1595**, 203-209.
3. Silva, J.L., Weber, G. (1993) Pressure stability of proteins, *Annual Review of Physical Chemistry* **44**, 89-113.
4. Mozhaev, V.V., Heremans, K., Frank, J., Masson, P., Balny, C. (1996) High pressure effects on protein structure and function, *Proteins-Structure Function and Genetics* **24**, 81-91.
5. Jonas, J., Jonas, A. (1994) High-pressure NMR-spectroscopy of proteins and membranes, *Annual Review of Biophysics and Biomolecular Structure* **23**, 287-318.
6. Gross, M., Jaenicke, R. (1994) Proteins under pressure. *Eur. J. Biochem.* **221**, 617-630.
7. Ernst, R.R. (2002) Preface. BBA Special Issue "Frontiers in high pressure biochemistry and biophysics", *Biochimica et Biophysica Acta* **1595**, 1-2.
8. Bartlett, D.H., Kato, C., Horikoshi, K. (1995) High-pressure influences on gene and protein expression, *Research in Microbiology* **146**, 697-706.
9. Lehninger, A.L. (1975) *Biochemistry,* Chapter 9, Worth Publishers, NY.
10. Thomanek, U.F., Parak, F., Mössbauer, R.L., Formanek, H., Schwager, P., Hoppe, W. (1973) Freezing of myoglobin crystals at high pressure, *Acta Cryst.* **A29**, 263-265.
11. Kundrot, C.E., Richards, F.M. (1987) Crystal structure of hen egg-white lysozyme at a hydrostatic pressure of 1000 atmospheres, *J. Mol. Biol.* **193**, 157-170.
12. Kundrot, C.E., Richards, F.M. (1986) Collection and processing of x-ray diffraction data from protein crystals at high pressure, *J. Appl. Cryst.* **19**, 208-213.
13. Katrusiak, A., Dauter, Z. (1996) Compressibility of lysozyme protein crystals by x-ray diffraction, *Acta Cryst.* **D52**, 607-608.
14. Fourme, R., Kahn, R., Mezouar, M., Girard, E., Hoerentrup, C., Prange, T., Ascone, I. (2001) High-pressure protein crystallography (HPPX): instrumentation, methodology and results on lysozyme crystals, *J. Synchrotron Rad.* **8**, 1149-1156.
15. Fourme, R., Ascone, I., Kahn, R., Mezouar, M., Bouvier, P., Girard, E., Lin, T., Johnson, J.E. (2002) Opening the high-pressure domain beyond 2 kbar to protein and virus crystallography, *Structure* **10**, 1409-1414.
16. Urayama, P., Phillips Jr., G.N., Gruner, S.M. (2002) Probing substates in sperm whale myoglobin using high-pressure crystallography, *Structure* **10**, 51-60.
17. Seddon, J.M., Templer, R.H. (1993) Cubic phases of self-assembled amphiphilic aggregates, *Phil. Trans. R. Soc. Lond. A* **344**, 377-401.
18. Seddon, J.M. (1990) Structure of the inverted hexagonal (H_{II}) phase, and non-lamellar phase transitions of lipids, *Biochimica et Biophysica Acta* **1031**, 1-69.

19. Gruner, S.M. (1994) Coupling between bilayer curvature elasticity and membrane protein activity, In *ACS Advances in Chemistry Series No. 235, Biomembrane Electrochemistry*ACS Books, Washington, DC.
20. Gruner, S.M. (1985) Intrinsic curvature hypothesis for biomembrane lipid composition: A Role for non-bilayer lipids, *Proc. Natl. Acad. Sci. USA* **82**, 3665-3669.
21. Gruner, S.M. (1989) Stability of lyotropic phases with curved interfaces, *J. Phys. Chem.* **93**, 7562-7570.
22. Gruner, S.M. (1991) Nonlamellar lipid phases, *Cell Membranes* **5**, 1-57.
23. Gruner, S.M. (1991) Lipid membrane curvature elasticity and protein function in L. Peliti (ed.), *Biologically Inspired Physics,* Plenum Press, New York, pp127-135.
24. Gruner, S.M. (1992) Nonlamellar Lipid phases, in P.L. Yeagle (ed.), *The Structure of Biological Membranes,* CRC Press, Boca Raton, FL, pp. 211-250.
25. Turner, D.C., Gruner, S.M., Huang, J.S. (1992) Distribution of decane within the unit cell of the inverted hexagonal (H_{II}) phase of lipid-water-decane systems using neutron diffraction, *Biochemistry* **31**, 1356-1363.
26. Tate, M.W., Gruner, S.M. (1989) Temperature dependence of the structural dimensions of the inverted hexagonal (H_{II}) phase of phosphatidylethanolamine containing membranes, *Biochemistry* **28**, 4245-4253.
27. So, P.T.C. (1992) *High pressure effects on the mesophases of lipid-water systems*, Ph.D. thesis, Dept. of Physics, Princeton University, Princeton, NJ.
28. Narayan, O., So, P.T.C., Turner, D.C., Gruner, S.M., Tate, M.W., Shyamsunder, E. (1990) Volume constriction in a lipid-water liquid crystal using high-pressure x-ray diffraction, *Phys. Rev. A.* **42**, 7479-7482.
29. So, P.T.C., Gruner, S.M., Shyamsunder, E. (1992) High-pressure dilatometer, *Rev. Sci. Instrum.* **63**, 5426-5431.
30. So, P.T.C., Gruner, S.M., Shyamsunder, E. (1992) Automated pressure and temperature control apparatus for x-ray powder diffraction studies, *Rev. Sci. Instr.* **63**, 1763-1770.
31. So, P.T.C., Gruner, S.M., Shyamsunder, E. (1993) Pressure induced topological phase transitions in membranes, *Phys. Rev. Lett.* **70**, 3455-3458.
32. Urayama, P.K. (2001) *Techniques for high pressure macromolecular crystallography and effects of pressure on the structure of sperm whale myoglobin*, Ph.D. thesis, Dept. of Physics, Princeton University, Princeton, NJ.
33. Epand, R.M. (1998) Lipid polymorphism and protein-lipid interactions, *Biochimica et Biophysica Acta* **1376**, 353-368.
34. Gruner, S.M., Shyamsunder, E. (1991) Is the mechanism of general anesthesia related to lipid membrane spontaneous curvature? *Annals N.Y. Acad. Sci.* **625**, 685-699.
35. Kirk, G.L., Gruner, S.M. (1985) Lyotropic effects of alkanes and headgroup composition on the L_α – H_{II} lipid liquid crystalline phase transition: hydrocarbon packing versus intrinsic curvature, *J. de Physique* **46**, 761-769.

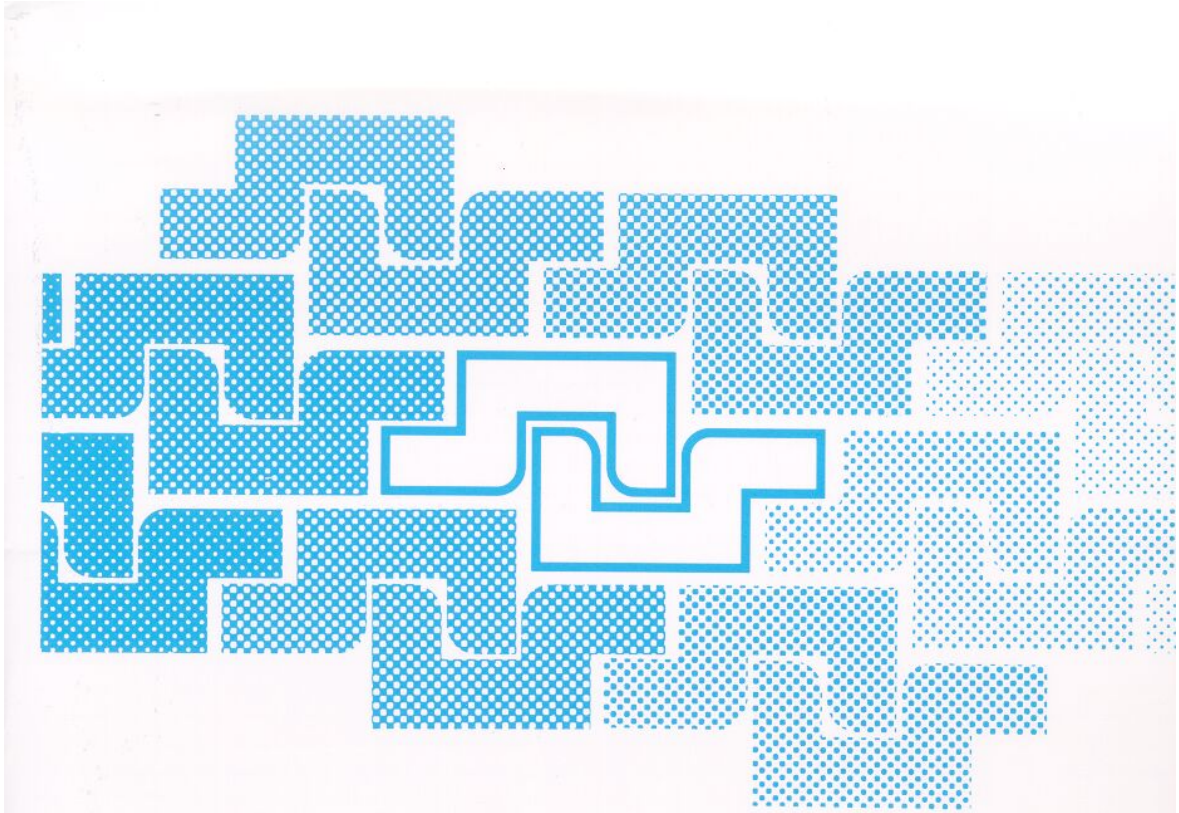

High-Pressure Crystallography

Edited by

Andrzej Katrusiak and Paul McMillan

NATO Science Series

II. Mathematics, Physics and Chemistry – Vol. 140

Proceedings of the NATO Advanced Research Workshop on
High-Pressure Crystallography
Erice, Italy
4–15 June 2003

A C.I.P. Catalogue record for this book is available from the Library of Congress.

ISBN 1-4020-1954-8 (PB)
ISBN 1-4020-1953-X (HB)
ISBN 1-4020-2102-X (e-book)

Published by Kluwer Academic Publishers,
P.O. Box 17, 3300 AA Dordrecht, The Netherlands.

Sold and distributed in North, Central and South America
by Kluwer Academic Publishers,
101 Philip Drive, Norwell, MA 02061, U.S.A.

In all other countries, sold and distributed
by Kluwer Academic Publishers,
P.O. Box 322, 3300 AH Dordrecht, The Netherlands.

Printed on acid-free paper

Printed in the Netherlands.